AN EXTENSION OF THIN-PLATE SPLINES FOR IMAGE REGISTRATION WITH RADIAL BASIS FUNCTIONS

Karl Rohr *Stefan Wörz*

University of Heidelberg, BIOQUANT, IPMB, and DKFZ Heidelberg,
Dept. Bioinformatics and Functional Genomics, Biomedical Computer Vision Group
Im Neuenheimer Feld 267, 69120 Heidelberg, Germany

ABSTRACT

Thin-plate splines are probably the most often used technique for landmark-based registration with radial basis functions. However, a disadvantage is that the locality of the transformation cannot be controlled. We introduce an extension of thin-plate splines which enables to control the spatial influence of acting forces and thus the locality of the transformation. Our approach is based on a new type of splines which we derived as closed-form solution of the biharmonic partial differential equation under certain forces. We have applied our approach to synthetic and real image data and have compared the results with standard thin-plate splines registration.

Index Terms— Deformable registration, non-rigid registration, thin-plate splines, landmark-based registration

1. INTRODUCTION

Since their invention about 40 years ago, *thin-plate splines (TPS)* have enjoyed widespread use for surface reconstruction and deformable image registration. The high popularity of these splines is due to the excellent interpolation properties, the physical motivation (minimization of a bending energy), the computational efficiency, and the ease of implementation. Moreover, TPS represent a closed-form solution of an energy functional, the mathematical theory is fully understood, and the uniqueness of the solution is guaranteed in practically all cases. In addition, the solution has a statistical interpretation as Bayes estimate (e.g., [9],[7]).

Originally, TPS have first been introduced in 1972 by Harder and Desmarais [5] in the context of aeroelastic calculations for surface interpolation. There, the term *surface splines* was used. Later, starting in 1976, mathematicians have laid the theoretical foundations of this approach and developed generalizations of it (Duchon [2], Wahba [9]). In this literature, TPS have also been denoted as *Duchon splines* or *Laplace splines*. In the field of image analysis, TPS were introduced for surface reconstruction given sparse scattered data in 1982 (e.g., Grimson [4]) and for landmark-based image registration in 1988 (e.g., Goshtasby [3], Bookstein [1]). At about the same time, TPS were also used in the field of computer graphics for surface interpolation and image warping (e.g., Wolberg [10]).

A main application field of TPS is image registration using a set of corresponding point landmarks. Landmark-based registration is computationally efficient and is applicable to monomodal and multimodal images. In addition, point landmarks are well-suited for user-interaction, which is important in clinical applications since physicians prefer to control the result. In comparison to rigid and affine registration, TPS enable deformable (non-rigid) registration and can cope with local geometric differences between images. However, a disadvantage is that the locality of the transformation cannot be controlled except by specifying additional landmarks, which is tedious and time-consuming. Another drawback stems from the fact that TPS are derived as solution of the biharmonic partial differential equation (PDE) from elasticity theory, where the landmarks are included as point forces. The forces are described by the Dirac delta function, which is zero everywhere, except at the origin where it has the value infinity. Therefore, the support of this function and thus the extent of the image regions on which the forces act, is infinitely small. An analogy is the pressing of a needle into a deformable material to generate the deformation. However, from a practical point of view, it is more reasonable that the forces act on regions with a larger support.

In this contribution, we introduce a new approach for deformable image registration based on an extension of TPS. In contrast to previous work, we suggest using smooth forces with a larger extent and which are represented by the Gaussian function. Under these forces, we derive a closed-form solution of the biharmonic PDE, which is a PDE of order four. It turns out, that the solution can be stated very compactly and allows straightforward use as radial basis function for spline-based registration. Since the Gaussian function is parameterized by its standard deviation, it is possible to control the spatial influence of the acting forces and thus the locality of the transformation. In addition, we show that the newly developed splines include TPS as a special case. Our work is related to TPS basis functions with compact support (e.g., [6],[8]). However, there the basis functions were de-

rived heuristically by truncating the original basis function at a certain value, which has a negative effect on the robustness (solvability of the linear system of equations). In addition, those basis functions do not represent a closed-form solution of a PDE. We have applied our registration approach to synthetic and real image data and we have performed an experimental comparison with the standard TPS approach.

2. THIN-PLATE SPLINES WITH GAUSSIAN FORCES FOR DEFORMABLE REGISTRATION

In this section, we first briefly describe the standard TPS approach for deformable image registration. Then, we derive the new class of thin-plate splines as closed-form solution of the biharmonic equation under Gaussian forces. We also study a limiting case of the resulting radial basis function and discuss the relation to the standard TPS basis function.

2.1. Thin-Plate Splines

Image registration based on TPS can be stated as a multivariate interpolation problem: Given a number n of corresponding point landmarks $\mathbf{p}_i$ and $\mathbf{q}_i$, $i = 1, \ldots, n$, in two images of dimension d, find a continuous transformation $\mathbf{u} : \mathbb{R}^d \rightarrow \mathbb{R}^d$ within a suitable Hilbert space $\mathcal{H}$ of admissible functions, which minimizes a certain functional $J : \mathcal{H} \rightarrow \mathbb{R}$ and fulfills the conditions $\mathbf{q}_i = \mathbf{u}(\mathbf{p}_i), i = 1, \ldots, n$, i.e., corresponding landmarks are mapped onto each other.

In the case of 3D images ($d = 3$), the TPS functional can be stated for each component $u_k, k = 1, \ldots, d$, of the transformation $\mathbf{u}$ as

$$J(u) = \iiint_{-\infty}^{\infty} u_{xx}^2 + u_{yy}^2 + u_{zz}^2 + 2(u_{xy}^2 + u_{xz}^2 + u_{yz}^2)\, d\mathbf{x},$$

where the subscripts denote partial derivatives w.r.t. the space coordinates and $d\mathbf{x} = dxdydz$. The functional is usually referred to as bending energy. For this minimization problem the solution is unique and can be stated in closed form ([2],[9]). The solution consists of polynomials and a superposition of certain radial basis functions $R(r)$, where $r = |\mathbf{x}|$, $\mathbf{x} = (x, y, z)$, and $|\cdot|$ is the Euclidean distance:

$$u(\mathbf{x}) = \sum_{\nu=1}^{M} a_\nu \phi_\nu(\mathbf{x}) + \sum_{i=1}^{n} w_i R(|\mathbf{x} - \mathbf{p}_i|) \tag{1}$$

with the monomials $\phi_\nu(\mathbf{x})$. The coefficients a_ν and w_i can be computed efficiently by solving a linear system of equations:

$$\begin{aligned} \mathbf{P}\mathbf{a} + \mathbf{K}\mathbf{w} &= \mathbf{v} \\ \mathbf{P}^T\mathbf{w} &= \mathbf{0}, \end{aligned} \tag{2}$$

where $\mathbf{a} = (a_1, \ldots, a_M)^T$, $\mathbf{w} = (w_1, \ldots, w_n)^T$, $\mathbf{K} = (K_{ij})$, $K_{ij} = R(|\mathbf{p}_i - \mathbf{p}_j|)$, $\mathbf{P} = (P_{ij})$, $P_{ij} = \phi_j(\mathbf{p}_i)$, and $\mathbf{v}$ is the column vector of one component of the coordinates of the landmarks $\mathbf{q}_i$. The uniqueness of the solution of the linear system of equations (2) is guaranteed under the very general condition that not all landmarks may lie on a single plane.

The radial basis function in (1) in the 3D case is

$$R_{TPS}(r) = -\frac{1}{8\pi}\, r \tag{3}$$

and is a Green's function of the biharmonic PDE, a fourth-order PDE from elasticity theory. Thus, $R_{TPS}(r)$ solves

$$\Delta^2 R_{TPS}(r) = \delta(r), \tag{4}$$

where Δ is the Laplacian operator, and $\delta(r)$ denotes the Dirac delta function which corresponds to the acting forces at the landmarks. The Dirac delta function has the value infinity at $r = 0$ (singularity at the origin) and is otherwise zero. The support of this function and thus the spatial region on which the forces act is infinitely small (point forces). An analogy is the pressing of a needle into a deformable material to generate the deformation. However, from a practical point of view, it is more reasonable to use forces which have a larger extent and which are smooth.

2.2. Gaussian Thin-Plate Splines

Instead of using point forces $\delta(r)$, which act on an infinitely small region as in the case of TPS, we here suggest using Gaussian forces for solving the corresponding minimization/PDE problem stated above. Gaussian forces are described by a Gaussian function parameterized with the standard deviation σ and they have several advantages over point forces. In particular, Gaussian forces act on larger regions and the spatial influence can be controlled by the standard deviation. In addition, they have a definite value at the origin, they are smooth, and they decrease fast to zero with increasing distance to the origin. In the 3D case, Gaussian forces can be written as

$$G(\mathbf{x}, \sigma) = G(r, \sigma) = \frac{1}{\sigma^3} G\Big(\frac{r}{\sigma}\Big), \quad G(r) = \frac{1}{\left(\sqrt{2\pi}\right)^3} e^{-\frac{r^2}{2}}.$$

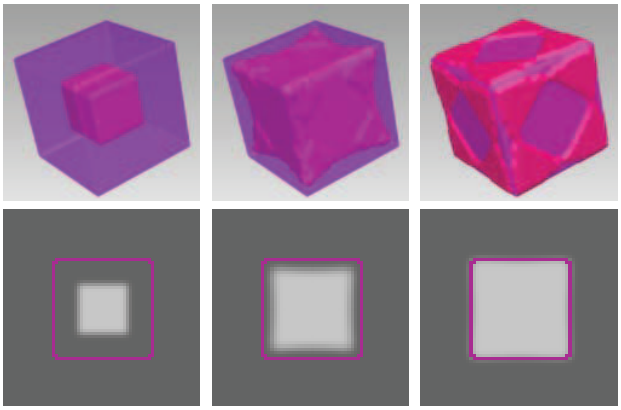
Compared to the PDE for TPS in (4), we here consider the problem

$$\Delta^2 R_{GTPS}(r) = G(r, \sigma). \tag{5}$$

We have derived the solution of this fourth-order PDE using the method of Green's function and found that the solution can be stated in compact form as:

$$R_{GTPS}(r) = -\frac{1}{8\pi}\left(4\pi\sigma\, G\Big(\frac{r}{\sigma}\Big) + \left(r + \frac{\sigma^2}{r}\right) \operatorname{erf}\left(\frac{r}{\sqrt{2}\sigma}\right)\right)$$

with the error function $\operatorname{erf}(r) = (2/\sqrt{\pi}) \int_0^r e^{-\xi^2} d\xi$. Since the derivation is based on Gaussian forces we use the term



Unregistered TPS GTPS

Fig. 1. Registration of 3D synthetic images: 3D visualizations (top) and 2D sections from the middle of the 3D images (bottom) for the unregistered case as well as for TPS and GTPS.

Gaussian thin-plate splines (GTPS) to refer to this type of splines. Compared to the TPS basis function in (3), the GTPS basis function is smooth, i.e., it has no kink at $r = 0$. GTPS can be directly used for image registration and the transformation can be computed efficiently based on a linear system of equations which has the same form as in the case of TPS in (2) above.

2.3. Limiting Case of the Basis Function

The most interesting limiting case of the GTPS basis function is when the parameter σ approaches zero. In this case we have

$$\lim_{\sigma \to 0} R_{GTPS}(r) = \lim_{\sigma \to 0} \left(-\frac{1}{8\pi}\, r\, \mathrm{erf}\left(\frac{r}{\sqrt{2}\sigma} \right) \right) = -\frac{1}{8\pi}\, r.$$

In fact, the result is identical to the TPS basis function in (3). Thus, for σ approaching zero, the GTPS basis function converges to the TPS basis function. This means that GTPS include TPS as a special case.

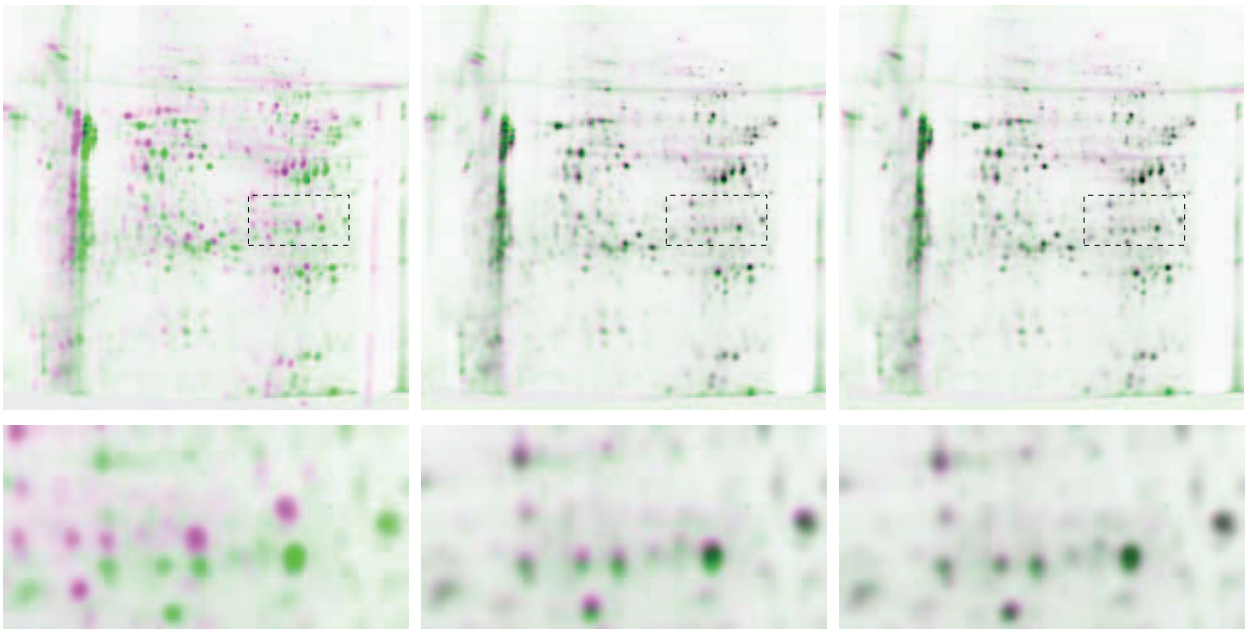
3. EXPERIMENTAL RESULTS

We have applied the GTPS approach for registration of synthetic and real image data, and have compared the results with the TPS approach. Fig. 1 shows the registration result of an experiment with 3D synthetic images of two cubes. We used eight landmarks at the corners of the 3D cubes as well as 26 regularly distributed landmarks at the 3D image border, which act as boundary conditions. The images have a size of $64 \times 64 \times 64$ voxels. Applying TPS, it can be seen that the surfaces of the 3D cubes are not well aligned. In comparison, using GTPS with the same landmarks and $\sigma = 10$ yields a much better registration result (see the 3D visualizations and corresponding 2D sections from the middle of the 3D images, and note that the bright red regions in the 3D visualization for GTPS represent a deviation of at most 1 voxel). We have also quantified the registration accuracy based on the Dice coefficient D using binary images. It turns out that while for the unregistered case we have $D = 0.21$, for TPS we obtain $D = 0.68$, and GTPS yield a significantly better result of $D = 0.97$. An optimal value for the standard deviation σ for GTPS was found as follows. We computed registration results for different values of σ (integer values starting from $\sigma = 1$) and chose the value for which the root mean squared intensity error (RMSE) between the two images is minimal while at the same time the determinant of the Jacobian matrix of the transformation is required to be positive (ensuring a one-to-one mapping).

Table 1. Quantitative results for gel electrophoresis images.

	Whole images			ROI		
	Dice	RMSE	$\Delta\%$	Dice	RMSE	$\Delta\%$
Unreg.	0.112	25.79		0.011	29.62	
TPS	0.603	14.43	+44.0%	0.587	13.33	+55.0%
GTPS	0.650	13.35	+48.2%	0.754	9.67	+67.3%

We have also applied our approach to register gel electrophoresis images which represent protein expression. Typically, images from a reference group are compared with those from a test group, e.g., before and after taking drugs to analyze the effect of medication. Due to complex physical and chemical processes the images are non-rigidly distorted. In our study, we used images which represent the effect of a plant extract on the protein expression of IBR3 human dermal fibroplasts. The images have a size of 1024×1024 pixels (the data is courtesy of G.-Z. Yang, Imperial College of Science, Technology, and Medicine, London/UK). As an example, Fig. 2 (left) shows a color overlay of two corresponding gel electrophoresis images (magenta, green). In the top row, the whole images are shown and in the bottom row an enlarged section (ROI) is displayed. It can be seen, that there exists a large discrepancy between the original images. Applying TPS gives an overall good registration result (Fig. 2, middle), however, a number of spots at the bottom and on the left are not well aligned (see the remaining magenta and green colored regions). In comparison, using GTPS yields a much better result and the spots at the bottom and on the left are well registered (hardly any magenta and green colored regions remain, and in nearly all regions grey tones can be observed), see Fig. 2 (right). We have also quantified the registration accuracy. While in the unregistered case, we have a Dice coefficient of $D = 0.11$, TPS yield $D = 0.60$, and GTPS achieve $D = 0.65$. GTPS improve the result by 7.8% compared to TPS. For the RMSE, GTPS improve the result by 6.4% compared to TPS, and 48.2% compared to the unregistered case (see Tab. 1). If we consider the performance within the ROI shown in Fig. 2, we obtain a better improvement. For the Dice coefficient, GTPS yield an improvement of 28.4% com-



Unregistered TPS GTPS

Fig. 2. Registration of gel electrophoresis images: Color overlays of whole images (top) and enlarged sections (bottom) for the unregistered case (left) as well as for TPS (middle) and GTPS (right).

pared to TPS. For the RMSE, GTPS yield an improvement of 27.5% compared to TPS, and 67.3% compared to the unregistered case (Tab. 1). The computation time for registering a pair of gel electrophoresis images with 1024×1024 pixels was about 1 sec for GTPS and TPS on a 2.67GHz Intel Xeon PC running Linux.

4. CONCLUSION

We have introduced a new approach for deformable image registration with radial basis functions. The approach is based on a new type of splines, which we derived as closed-form solution of the biharmonic PDE from elasticity theory under Gaussian forces. A main advantage of our approach is that the spatial influence of acting forces and thus the locality of the transformation can be controlled. We also showed that TPS are a special case of the new splines. Based on experimental results we found that our approach improves the registration result compared to TPS.

5. REFERENCES

[1] F.L. Bookstein, "Principal Warps: Thin-Plate Splines and the Decomposition of Deformations", *IEEE Trans. on Pattern Anal. and Mach. Intell.* 11:6 (1989) 567-585

[2] J. Duchon, "Interpolation des fonctions de deux variables suivant le principe de la flexion des plaques minces", *R.A.I.R.O. Anal. Numérique* 10:12 (1976) 5-12

[3] A. Goshtasby, "Registration of Images with Geometric Distortions", *IEEE Trans. on Geoscience and Remote Sensing* 26:1 (1988) 60-64

[4] W.E.L. Grimson, "A Computational Theory of Visual Surface Interpolation", *Phil. Trans. R. London* B 298 (1982) 395-427

[5] R.L. Harder and R.N. Desmarais, "Interpolation Using Surface Splines", *J. of Aircraft* 9 (1972) 189-191

[6] J. Li, X. Yang, J. Yu, "Compact Support Thin Plate Spline Algorithm", *J. of Electron.* 24:4 (2007) 515-522

[7] K. Rohr, *Landmark-Based Image Analysis: Using Geometric and Intensity Models,* Kluwer Academic Publishers, Dordrecht Boston London 2001

[8] W. Sun, X. Liu, X. Yang, "Non-rigid Registration Using Robust Point Matching with Compactly Supported Radial Basis Function", *J. of Computational Information Systems* 6:9 (2010) 2983-2989

[9] G. Wahba, *Spline Models for Observational Data,* Society for Industrial and Applied Mathematics, Philadelphia, Pennsylvania, 1990

[10] G. Wolberg, *Digital Image Warping,* IEEE Computer Society Press Washington 1990